Reactive Compensation Planning in Unbalanced Electrical Power Systems

Jair Salazar [1],*[ID], Diego Carrión [2][ID] and Manuel Jaramillo [2][ID]

1   Master's Program in Electricity, Salesian Polytechnic University, Quito EC170702, Ecuador
2   Smart Grid Research Group—GIREI (Spanish Acronym), Salesian Polytechnic University,
     Quito EC170702, Ecuador
*   Correspondence: jsalazarl3@est.ups.edu.ec

Abstract: This research focuses on finding the optimal location of reactive compensation in an unbalanced electrical power system (EPS). An EPS is named unbalanced when there is uncertainty in the behaviour of the power demand, which causes changes in the voltage profile and angle of each of the electrical power phases. For this reason, using reactive compensation will improve the voltage profiles and the magnitudes of reactive power in the transmission lines. The proposed methodology uses the optimal AC power flows as a basis, which is applied to each power phase and, through this methodology, the operating conditions of the EPS are determined. Then, based on the voltage profiles of each power phase, it was possible to determine the critical nodes of the system, so that afterwards, through heuristics, it was possible to find the optimal location of the reactive compensation that independently meets the needs of each phase. To evaluate the proposed methodology, the IEEE test systems of 9, 14, 30 and 118 bus bars were used, as well as the 230 kV ring of the Ecuadorian transmission system. Finally, using the proposed methodology, it was possible to independently compensate for each of the power phases, rectifying the unbalanced voltage profiles that appeared in the EPS.

Keywords: reactive compensation; optimal power flow; electrical power-system planing; unbalanced systems; optimal location

1. Introduction

1.1. Research Background

The planning of an electrical power system fulfills an important function because as the years go by the growth in demand is clear. In order to cover the requirements of voltage levels, the authors in [1,2] propose the use of reactive compensation and an algorithm that differentiates multi-objective optimization problems (MOP) which offer more realistic values, where losses in transmission lines are reduced so that as demand grows, voltages can be maintained in optimal conditions.

There are different ways to perform optimal control in electrical power systems; these include adjusting the tap of the transformer, and the generation of reactive power (var), among others. Therefore, it is a challenge to include reactive power planning (RPP). Consequently, a two-level strategy is proposed in order to reduce the cost of operation related to the problem of RPP [3].

1.2. Literature Review

In [4], a management strategy of reactive power in transmission–distribution is proposed through a network planning approach; that planning largely depends on rules and requirements to be able to count on the support of distributed generation (DG).

The systematic approach to a dynamic optimal resource (var) scheduling and updating, where very few have combined installation and removal together, comes from a load-side

strategy (LSC) and an induction generator for stability improvement. This is designed using the adaptive sliding mode method (SM) [5–7].

In [8], a reactive power dispatch (RPD) is proposed employing a bee-colony algorithm which is based on minimizing active power losses using a mixed-integer linear optimization to find the configuration of the variables of control.

A planning strategy is the main study that allows examination of the impact of multiple uncertainties, where it tries to immunize reactive power planning against variations in demand in the presence of multiple targets since it employs a high degree of parallelization which is based on a meta-heuristic population to obtain a manageable solution. Thus, planning systems are given a systematic way to determine the optimal size, location and type of compensation, ensuring a reduced investment cost [9,10].

All compensation devices have operating limits; these devices can be STATCOM, SVC, TCR, SSSC and TCSC and when there is a network failure these devices are outside the permitted ranges since they are designed to operate within specified ranges [11]. The location and installation of FACTS depend on operative variables, since they allow for the expansion or improvement of the viability of the domain for the system and in the long term. In addition, they allow savings in operative expenses and have a cheaper generation than using a heuristic algorithm to solve the non-convex optimization problem [12].

Currently, several authors have focused on developing methodologies for the location of FACTS devices, for example in [13] the authors proposes an optimal multi-objective location of series compensators in transmission lines using a heuristic methodology. In the same way, in [14], a hueristic methodology is proposed for the optimal location of SVC and TCSC, in order to improve the control of power flows in the EPS.

The work in [15] includes the probabilistic reliability criterion, which is entered as a constraint in the reliable-economic co-planning solution and is solved through mixed-integer programming.

To maximize the voltage collapse range, an optimization problem is formulated using reactive energy injections subject to power-flow restrictions and voltage operation, where the reactive power compensation takes into account the maximum active power arriving at a linear approximation and convex reformulation by variation in power-flow equations [16,17].

The capacitor banks connection forms and a new method of reactive compensation are given in [18]. In [19], the research presents the application of a hybrid algorithm which makes it possible to determine the best size and location for fixed and switching capacitors in electrical networks.

The reactive power-planning methodology also helps to recover from failures and improve the voltage level after a contingency; it is based on the application of the optimal reactive power-planning problem considering voltage stability as the initial solution of the problem of fuel cost minimization [20,21]. The reconfiguration of the reactive flows in the EPS is one of the additional advantages after the implementation of FACTS devices, studies such as [22] analyze the reconfiguration of power flows and [23] the dispatch of reactive power.

Fractal search (FSA) assists in the optimal reactive power distribution of static var compensation (SVC) devices and reconfiguration of multiple breakers installed in specific locations in coordination with transformers to minimize total loss and reduce voltage drop considering demand growth [24].

There are two scenarios to be considered, under-compensation and overcompensation, both dependent on the power of the corresponding loads, and they help to identify where the initial compensation can be changed or adjusted in order to improve the operation of the transformers, for which the predictive finite control set model is applied for dynamic reactive power compensation through an active-power hybrid filter [25,26].

It is possible to obtain a better net cost–benefit in the compensation coefficient by evaluating the feeder failure rate with hybrid algorithms [27]. Ref. [28] proposes a study

with two levels, where the upper level seeks to minimize the cost of the unbalanced network and the lower level aims to minimize energy losses and voltage imbalance.

When there is a very high level of renewable-energy penetration, an optimization based on multi-objective teaching and learning is proposed for the location of static compensators and to be able to minimize the power of the network; on the other hand, to be able to carry out the load uncertainty model, it is necessary to apply fuzzy-use-data theory, which allows Pareto optimal results [29,30].

Unbalanced electrical phases in a power system do not allow efficient energy delivery; thus, one of the solutions is a linear load flow where the ZIP model is considered in the loads with a sensitivity matrix that is studied for any variation in the voltage on all three phases [31–33].

In [34], the author proposes a series of simulations on bus-bar specified by the Monte Carlo method when there is unbalanced voltage profiles using the three-phase Newton Raphson methodology taking into consideration historical data when there is no more information on load tracking.

1.3. Research Contribution

This article proposes the location of reactive compensation to correct unbalanced electrical phases in the EPS. This process is developed starting with the EPS analysis through optimal AC power flows, which will help to determine the magnitudes of voltage profile in each bus bar and then, by finding a deficient bus bar, the compensation will be carried out. The proposed model can also be fulfilled in any EPS when there is an extension of it, and is able to execute the power flow. Starting from a bibliographic review and technological surveillance throughout the investigation, to identifying the conditions, variables involved and methods applied which are adjusted to the exposed needs, the different proposals will be analyzed and knowledge gaps, where it is possible to contribute with this research, will be identified, see Figure 1.
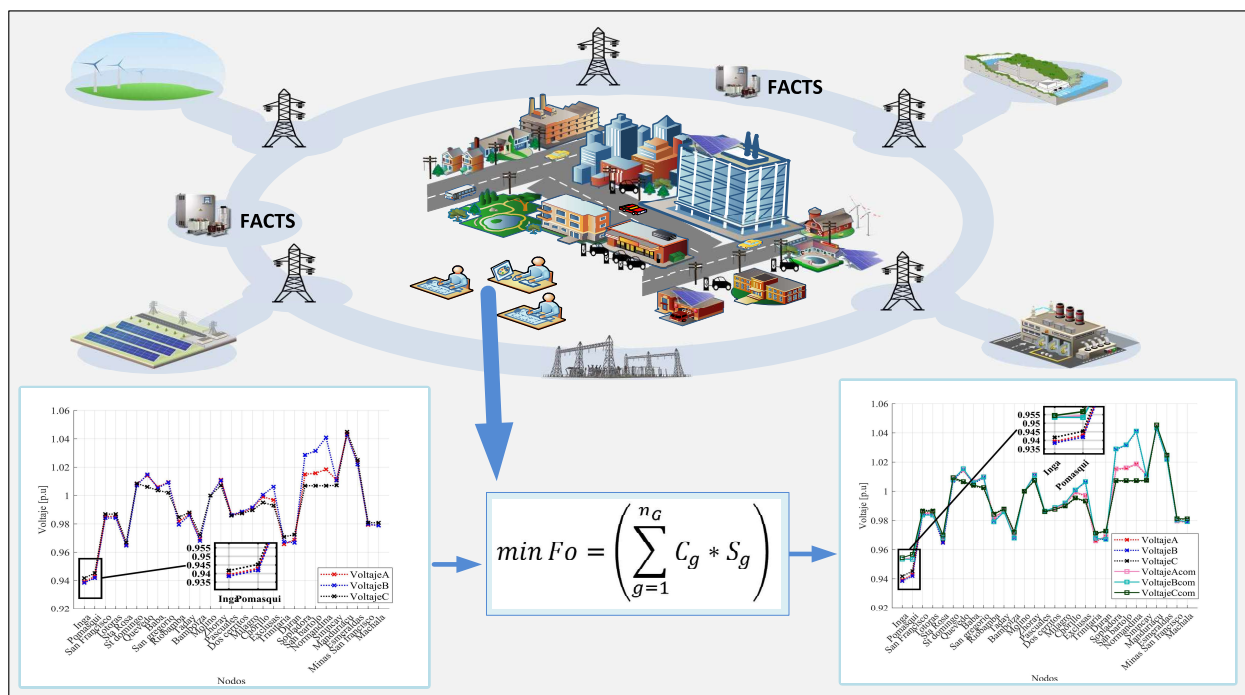

$$min\, Fo = \left(\sum_{g=1}^{n_G} C_g * S_g \right)$$

Figure 1. Reactive compensation architecture under unbalanced flows conditions.

2. Related Works

2.1. Multiple Compensations in Power Flow

The representation between the bus and the compensator is described in Figure 2, which shows the exchange of active and reactive power when there are multiple devices [11,35].
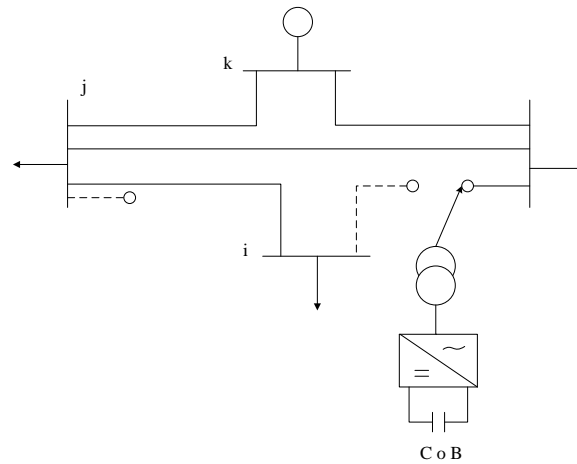

Figure 2. Multiple compensations in an EPS.

Equations (1) and (2) are the initial and fundamental parts to include in reactive compensation in the power flow.

$$P_{sh} = V_i^2 G_{sh} - V_i V_{sh}(G_{sh}cos(\theta_i - \theta_{sh})$$
$$- B_{sh}sen(\theta_i - \theta_{sh})) \tag{1}$$
$$Q_{sh} = -V_i^2 G_{sh} - V_i V_{sh}(G_{sh}sen(\theta_i - \theta_{sh})$$
$$- B_{sh}cos(\theta_i - \theta_{sh})) \tag{2}$$

The exchange of active power (PE) is given in Equation (3), where it must be ensured that the exchange of net active power is zero or close to zero so that the maximum flow of reactive power occurs.

$$PE = P_{sh}$$
$$= V_i^2 G_{sh} - V_i V_{sh}(G_{sh}cos(\theta_i - \theta_{sh})$$
$$- B_{sh}sen(\theta_i - \theta_{sh})) = 0 \tag{3}$$

Equation (4) is the reactive power control to the connected bus, also as indicated in Equation (2). Through Equations (5) and (6), the voltage is calculated at the node where the compensation is connected, which corresponds to the reactance balance shown in (7).

$$Q_{sh} - Q_{sh}^{spec} = 0 \tag{4}$$

$$V_i - V_i^{spec} = 0 \tag{5}$$

$$V_{sh} - V_{sh}^{spec} = 0 \tag{6}$$

$$X_{ij} - X_{ij}^{spec} = 0 \tag{7}$$

The current control can be leading or lagging; Equation (8) shows the capacitive form and (9) shows the inductive form.

$$Re(I_{sh}^{spec} \angle (\theta_{sh} + 90°)) = Re((V_i - V_{sh})/Z_{sh})$$
$$\Rightarrow Im(I_{sh}^{spec} \angle (\theta_{sh}^{spec} + 90°))$$
$$= Im((V_i - V_{sh})/Z_{sh}) \tag{8}$$

$$Re(I_{sh}^{spec} \angle (\theta_{sh} - 90°)) = Re((V_i - V_{sh})/Z_{sh})$$
$$\Rightarrow Im(I_{sh}^{spec} \angle (\theta_{sh}^{spec} - 90°))$$
$$= Im((V_i - V_{sh})/Z_{sh}) \tag{9}$$

Equation (10) show the control for apparent power and Equation (11) shows the control in general.

$$S_{ij} - S_{ij}^{spec} = 0 \tag{10}$$

$$\Delta E(x) = E(x) - E(x)^{spec} \tag{11}$$
$$x = [\theta_i, V_i, \theta_{sh}, V_{sh}]$$

In Equation (12), the Jacobian of the power system is shown where the derived active and reactive power functions are considered concerning the state variables in the voltage and angle at the nodes, which allows the values of the state variables to be determined by Equation (13).

$$[J] = \begin{bmatrix} \frac{\partial P_i}{\partial \theta_i} & \frac{\partial P_i}{\partial V_i} & \frac{\partial P_i}{\partial \theta_{sh}} & \frac{\partial P_i}{\partial V_{sh}} \\ \frac{\partial Q_i}{\partial \theta_i} & \frac{\partial Q_i}{\partial V_i} & \frac{\partial Q_i}{\partial \theta_{sh}} & \frac{\partial Q_i}{\partial V_{sh}} \\ \frac{\partial PE}{\partial \theta_i} & \frac{\partial PE}{\partial V_i} & \frac{\partial PE}{\partial \theta_{sh}} & \frac{\partial PE}{\partial V_{sh}} \\ \frac{\partial E}{\partial \theta_i} & \frac{\partial E}{\partial V_i} & \frac{\partial E}{\partial \theta_{sh}} & \frac{\partial E}{\partial V_{sh}} \end{bmatrix} \tag{12}$$

$$\begin{bmatrix} \Delta \theta_1 \\ . \\ . \\ . \\ \Delta \theta_{N-1} \\ \Delta V_1 \\ . \\ \Delta V_{N-1} \\ \Delta \theta_{sh} \\ \Delta V_{sh} \end{bmatrix} = -([J])^{-1} \begin{bmatrix} \Delta P_1 \\ . \\ . \\ . \\ \Delta P_{N-1} \\ \Delta Q_1 \\ . \\ . \\ \Delta Q_N \\ \Delta PE \\ \Delta E \end{bmatrix} \tag{13}$$

In addition, with the process described above, it is also possible to determine the dispatches of active and reactive power of the generators, which are calculated using Equations (14) and (15), respectively. The balance of active and reactive power in each node is calculated with Equations (16) and (17), respectively. In addition, finally, Equations (18)–(21) allow calculation of the power balance in the EPS.

$$P_i = P_i^{gen} - P_i^{carga} \tag{14}$$

$$Q_i = Q_i^{gen} - Q_i^{carga} \tag{15}$$

$$P_i^{cal}(x) = \sum_{j}^{N} V_i V_j (G_{ij} cos(\theta_i - \theta_j) + B_{ij} sen(\theta_i - \theta_j)) \tag{16}$$

$$Q_i^{cal}(x) = \sum_{j}^{N} V_i V_j (G_{ij} sen(\theta_i - \theta_j) - B_{ij} cos(\theta_i - \theta_j)) \tag{17}$$

$$\Delta P_i = P_i - P_i^{cal}(x) \tag{18}$$

$$\Delta Q_i = Q_i - Q_i^{cal}(x) \tag{19}$$

$$\Delta E = E(x) - E(x)^{spec} \tag{20}$$

$$\Delta PE = PE(x) - PE(x)^{spec} \tag{21}$$

2.2. Stochastic Model That Considers Uncertainties in Demand

The model described below presents the stochastic optimization planning that takes into account the uncertainty of the demand; therefore, from Equation (22) to (25), an abstract formulation is presented where (x) is a binary vector and means the inversion of the candidate sites, (y) is also a binary vector which represents auxiliary binaries in the constraints of the system and (z) represents the power shipments to the system.

The objective function is described in Equation (22), which seeks to minimize the cost of investment and the operation of the system, which is subject to (23) where (x) and (y) are presented in binary form, Equation (24) shows the investment constraint and Equation (25) shows the operation constraint [15,36].

$$\min a^T x + f^T z \tag{22}$$

$$s.t. \, x, y \in \{0, 1\} \tag{23}$$

$$Ax \leq m \tag{24}$$

$$g(x, y, z) \leq n \tag{25}$$

The proposed model presents predicted information to calculate operating costs and cover uncertainties, in which Equation (26) penalizes load shedding, which is included in Equations (27) and (28) to present the balance in different cases, and in Equation (29) the model saves the different annual disconnections with their respective restriction in Equation (30).

$$\min CI + CO + C^{loss} + \rho^{\xi} \sum_t \Delta D_t^{\xi} \tag{26}$$

$$\sum_{g \in \Omega j} P_{ght}^{\xi} + \sum_{w \in \Omega j} P_{wht}^{\xi} - \sum_{d \in \Omega j} (P_{dht}^{\xi} - \delta_{dht}^{\xi})$$

$$= \sum_{(i,j) \in \Omega j} P_{ij,ht}^{\xi} - \sum_{(j,k) \in \Omega j} P_{jk,ht}^{\xi} \tag{27}$$

$$\sum_{g \in \Omega j} Q_{ght}^{\xi} - \sum_{d \in \Omega j} (Q_{dht}^{\xi} - (\delta_{dht}^{\xi}/P_{dht}^{\xi})Q_{dht}^{\xi}) + \sum_{b \in \Omega j} Q_{bht}^{\xi}$$

$$+ \sum_{sh \in \Omega j} Q_{shht}^{\xi} = \sum_{(i,j) \in \Omega j} Q_{ij,ht}^{\xi} - \sum_{(j,k) \in \Omega j} Q_{jk,ht}^{\xi} \tag{28}$$

$$\Delta D_t^{\xi} = \sum_h \sum_d T_{ht} \delta_{dht}^{\xi} \tag{29}$$

$$\Delta D_t^{\xi} \leq \Delta D_t^{max} \tag{30}$$

Equation (31) is the extended form of Equation (26) where the objective is to seek a minimum cost of operation of the base case and obtain a dispatch of the same case in the face of uncertainties, with different scenarios; from then on, the restrictions in Equations (34) and (35), which determine the limitations of uncertain scenarios such as the base case and the uncertainty of these scenarios, are coupled with the capacity of the generation centres, presented in Equation (36).

$$min \ a^T x + f_1^T z^b + \sum_\xi \rho^\xi f_2^T \delta^\xi \tag{31}$$

$$s.t. \ x, y^b y^\xi \in \{0,1\} \tag{32}$$

$$Ax \le m \tag{33}$$

$$g(x, y^b, z^b) \le n \tag{34}$$

$$g(x, y^\xi, z^\xi, \delta^\xi) \le n \tag{35}$$

$$Cz^b + Dz^\xi \le \Delta \tag{36}$$

2.3. Reactive Compensation Planning

The purpose of the objective function presented in Equation (37) is to recover the operation of the EPS after failures at the lowest possible cost, and to minimize the implementation of SVC and the energy losses in power lines [20,37].

$$min \ f1(x) = TVF_s \tag{37}$$

The minimisation of SVC is presented in Equation (38), which complements (37), which allows minimising losses and maintaining the stable operation of the power system by controlling the reactive power. This study is carried out dynamically and, for this, a response of this style is required from the SVCs and generators, which is restricted using Equation (39).

$$min \ f2(x) = C_e \zeta P_{loss} + \frac{1}{T_l} \sum_{i \in \Re_{SVC}} (C_{SVC}, iQ_{SVC}, i + F_{SVC}, i) \tag{38}$$

$$\begin{Bmatrix} x = f(x, y, u) \\ g(x, y, u) = 0 \end{Bmatrix} \tag{39}$$

The initial conditions of the study are shown in (40) for the case of the generators and, using (41) and (42), the active and reactive power of the generators at time t is determined. As for the reactive power of the SVC, it is defined in (43) where it depends on the time t and the angular frequency ω.

$$g(x_0, y_0, u_0) = 0 \tag{40}$$

$$P_{i,t}^G = \frac{E_i V_{i,t}}{X'_{d,i}} sen(\delta_{i,t} - \theta_{i,t}) \tag{41}$$

$$Q_{i,t}^G = \frac{E_i V_{i,t}}{X'_{d,i}} cos(\delta_{i,t} - \theta_{i,t}) - \frac{(V_{i,t})^2}{X'_{d,i}} \tag{42}$$

$$Q_{i,t}^{SVC} = (wC - \frac{2\beta_t - sen2\beta_t}{\pi \omega L})V_{i,t}^2 \tag{43}$$

3. Problem Formulation

To achieve the unbalanced flow model solution, it is proposed to use the optimal AC power flow model (OPF-AC), considering that the optimization must be applied independently for each of the phases and, in this way, the variables of voltage in the nodes and the power flows in each transmission line, generators and SVC obtained.

3.1. Optimal Power Flow—AC

The optimization model that allows determining the optimal AC power flows responds to a nonlinear optimization case (NLP); the objective function is presented in (44), where the costs of the generators are represented by (45).

$$min\ FO = \left(\sum_{g=1}^{n_G} C_g * S_g \right) \tag{44}$$

$$C_g * S_g = a_g * S_g^2 + b_g * S_g + c_g; \forall\, g\, \in\, n_G \tag{45}$$

The optimization model is restricted by (46) and (47), which represent the balance between generated and demanded power, while the power flows through the transmission lines are defined by (48) and (49). The operating limits of the system are the active and reactive power of the generators, the voltage and angle of the nodes are presented in (50), (51), (52) and (53), respectively.

$$P_g - P_D = \sum_{i=1}^{n_{bus}} P_{i,j}; \forall\, i, j\, \in\, n_{bus} \tag{46}$$

$$Q_g - Q_D = \sum_{i=1}^{n_{bus}} Q_{i,j}; \forall\, i, j\, \in\, n_{bus} \tag{47}$$

$$\begin{aligned} P_{ij} = |V_i|^2 G_{ij} - |V_i||V_j| [G_{ij} cos(\theta_i - \theta_j) \\ + B_{ij} sen(\theta_i - \theta_j)]; \forall\, i, j\, \in\, n_{bus} \end{aligned} \tag{48}$$

$$\begin{aligned} Q_{ij} = |V_i|^2 G_{ij} - |V_i||V_j| [G_{ij} sen(\theta_i - \theta_j) \\ + B_{ij} cos(\theta_i - \theta_j)]; \forall\, i, j\, \in\, n_{bus} \end{aligned} \tag{49}$$

$$P_g^{min} \le P_g \le P_g^{max}; \forall\, g\, \in\, n_G \tag{50}$$

$$Q_g^{min} \le Q_g \le Q_g^{max}; \forall\, g\, \in\, n_G \tag{51}$$

$$\left| V_i^{min} \right| \le V_i \le |V_i^{max}|; \forall\, i\, \in\, n_{bus} \tag{52}$$

$$\theta_{ij}^{min} \le \theta_{ij} \le \theta_{ij}^{max}; \forall\, i, j\, \in\, n_{bus} \tag{53}$$

$$\theta_{ij} = \theta_i - \theta_j \tag{54}$$

3.2. Study Cases

The proposed methodology was applied in the IEEE test models of 9, 14, 30 and 118 bus bars taking this as a starting point and then applying it to a real electrical system which will be the 230 kV system of Ecuador, as shown in Figure 3 and Table 1 [38].

Figure 4 shows the flowchart of the proposed methodology for reactive compensation in unbalanced systems. The proposed methodology objective is the improvement in the operability of the EPS through reactive compensation when there is uncertainty in demand, an action that frequently occurs, causing unbalanced flows. The voltage levels were also verified, as well as the reactive power dispatch of the generators, in the same way as the power Q in the transmission lines. Thus, the analysis was performed in different scenarios to demonstrate the effectiveness of the algorithm; however, the base points were the optimal power flows in AC (OPF-AC) which allows the obtaining of the magnitudes of each variable that was to be analyzed in order to later propose the compensation location through a heuristic, that is, it may be feasible without affecting the power system drastically and also without altering other magnitudes that may be important.
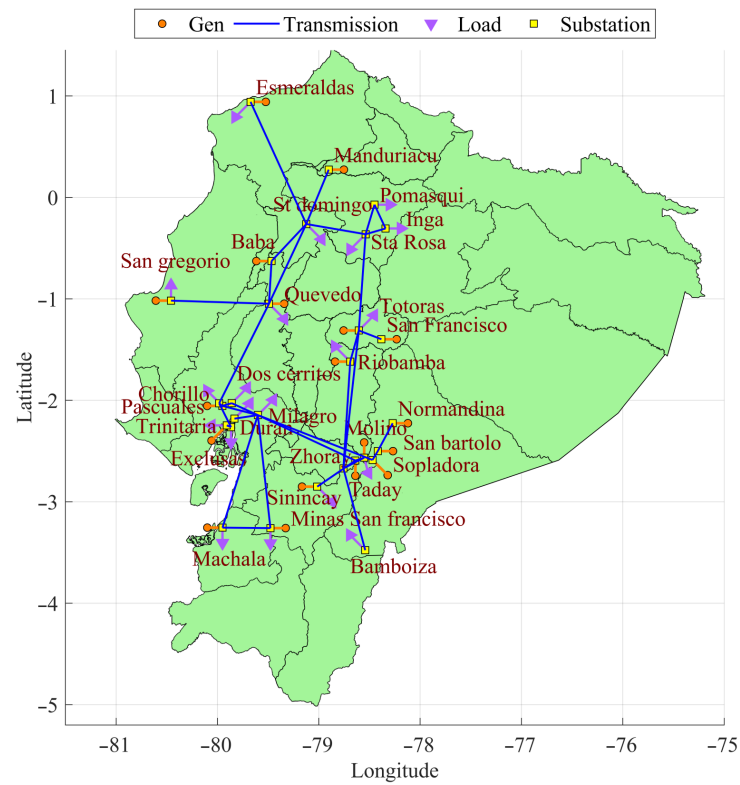
Figure 3. Ecuador electric system: 230 kV.

Table 1. Substation name with its reference number.

| #	Substation	#	Substation
1	Inga	16	Dos cerritos
2	Pomasqui	17	Milagro
3	San Francisco	18	Chorillo
4	Totoras	19	Exclusas
5	Sta Rosa	20	Trinitaria
6	St domingo	21	Duran
7	Quevedo	22	Sopladora
8	Baba	23	San bartolo
9	San gregorio	24	Normandina
10	Riobamba	25	Sinincay
11	Taday	26	Manduriacu
12	Bamboiza	27	Esmeraldas
13	Molino	28	Minas San francisco
14	Zhoray	29	Machala
15	Pascuales		
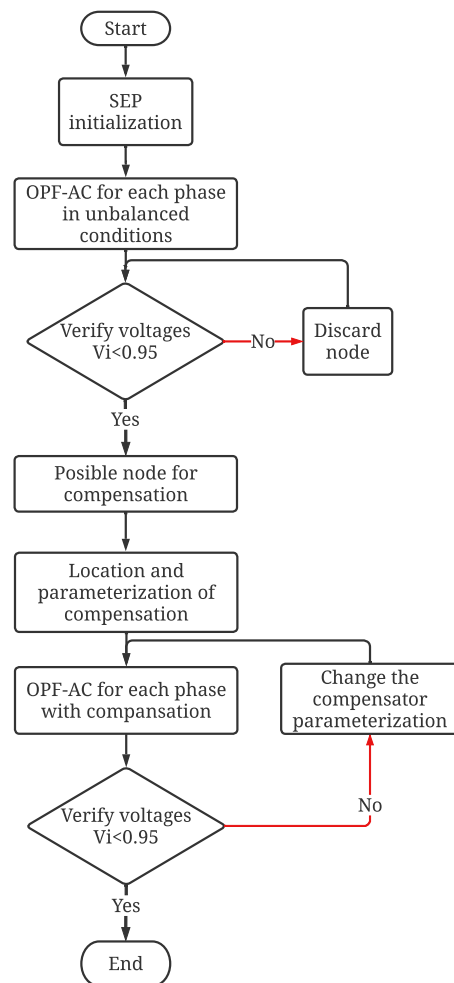
Figure 4. Flowchart of location of reactive compensation in unbalanced flow.

4. Analysis of Results

The following section presents the results achieved by the proposed methodology. What is presented below are the results of the optimal power flow with unbalanced loads and when reactive compensation is included. For this reason, the methodology is first analyzed in the IEEE test systems of 9, 14, 30 and 118 bus bars, respectively, and then in a real system. The variables that were taken into account were: voltage, reactive power dispatch of the generators and the flow in the transmission lines, achieving a contribution to the research field of reactive compensation against imbalance due to the action of uncertainty in demand.

4.1. Results on IEEE Test Systems

For the 9 bus bars test system, the node with the greatest problem is node 5, as it is the node of analysis since before compensation the unbalance is clear because the three phases have different magnitudes and are below 0.95 p.u., but after compensation, their magnitudes (of the three phases) are equalized, thus correcting the imbalance and obtaining a voltage improvement, as shown in the Figure 5. Therefore, the proposed model provides a significant contribution due to its compliance with what is proposed and reveals the deficiencies that can occur in electric systems.

For the 14 bus bar test system, no compensation is needed; nevertheless, it was implemented in node 14 to analyze the behaviour of the methodology, as can be seen in Figure 5. In the case of the 30 bus bar system, the model found 2 bars with drawbacks, which are nodes 14 and 30 where, after compensation, an improvement in voltage levels was achieved. In the case of 118 bus bars, compensation was located at node 118, where

there was also an improvement. The compensation values used in the study cases are detailed in Table 2; in Figure 5 it is visualized how the unbalance of the voltage of the phases was eliminated; in Figure 6 the response of the angle of the voltage for each phase is shown and in Figure 7 the dispatch of reagents of the generators.
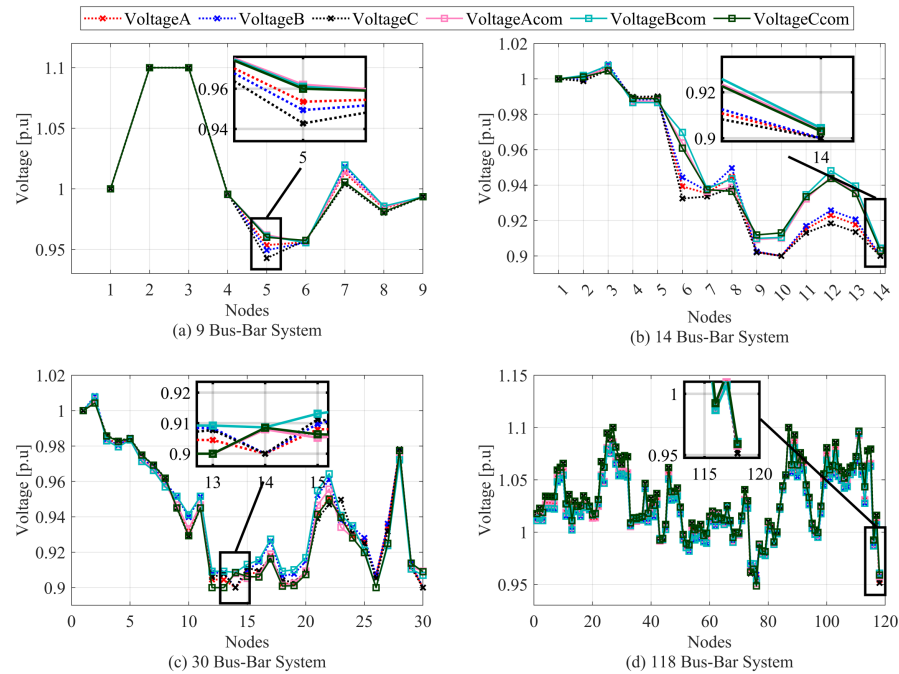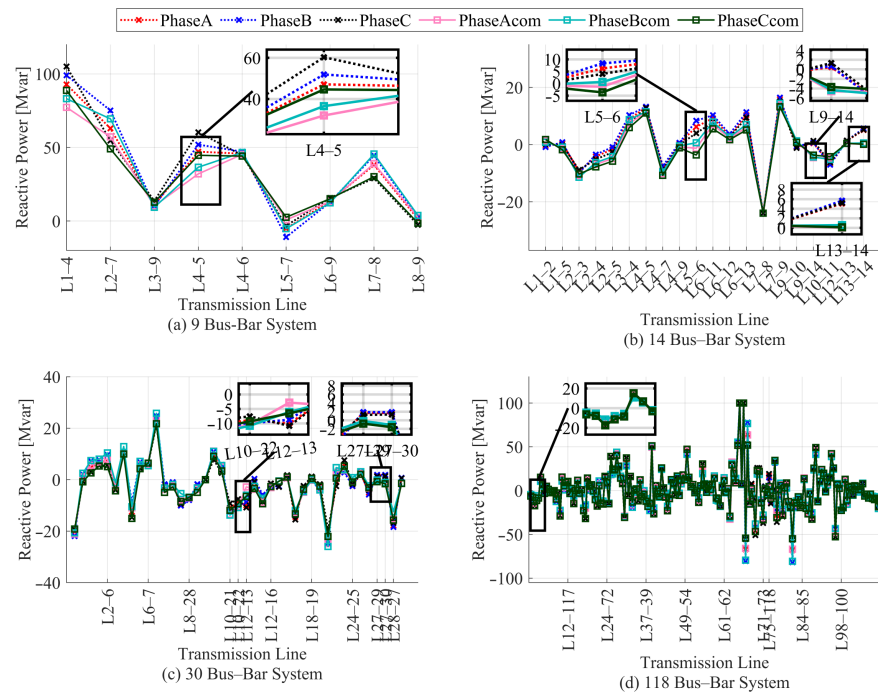

Figure 5. Voltage magnitude.
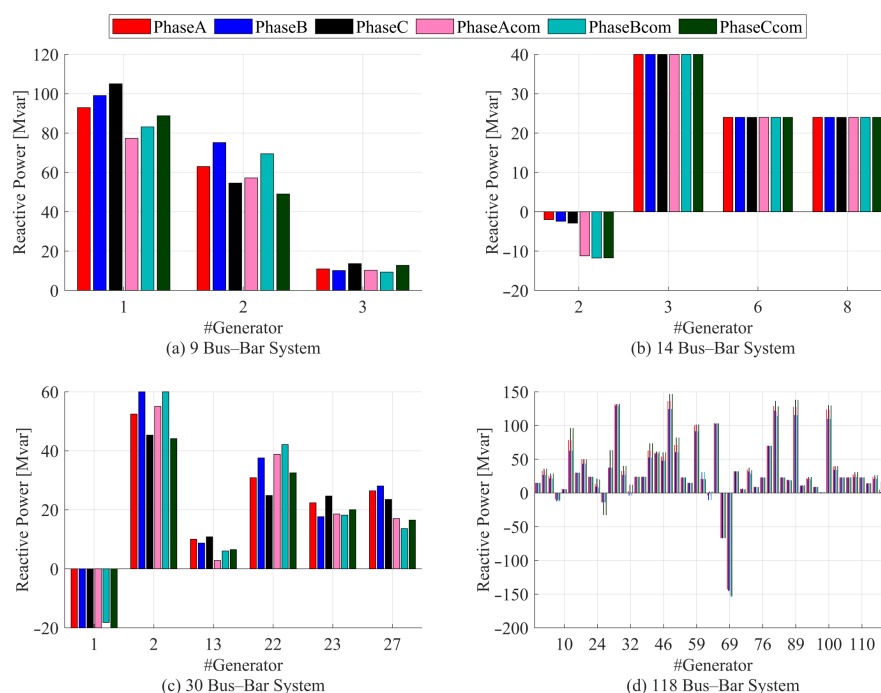

Figure 6. Transmission lines' reactive power.

Figure 7. Dispatch of reactive power from generators.

The voltage variation range is ±10% where the reference is 1 p.u, so the minimum would result in 0.9 and the maximum 1.1. The range of the angle would be the maximum of 0.6 and the minimum -0.6 radians, the stability values and the ranges considered by the OPF-AC.

The behaviour of the power flow of the transmission line is defined by Figure 6 and is given as the result of the optimal flow without compensation compared to when it was located, where, depending on the location of the compensation, the variation in the same is more clearly given by the change in reactive power value. For the 9 bus bar system, the compensation affects line 4–5, so it is correct since the compensation occurred in bar 5. For the 14 bus bar system, the affected lines are 5–6, 9–14 and 13–14, complying with the mathematical model because the compensation occurred in bar 14. For the 30 bus bar system, line 12–13 and line 27–30 had their values affected when compensation was made, but to a small extent, and, finally, in the 118 bus bar system, the affected line was 75–118. Everything mentioned is depicted in Figure 6.

Table 2. Reactive compensation values (Mvar).

System IEEE	Node Location for Compensation	Value [Mvar]
9	5	20
14	14	10
30	14	5
	30	5
118	118	20

The dispatch of reactive power by the generators can be seen in Figure 7, which shows how much reactive power each one delivers when there is compensation and when there is not, where the slack bar of the systems 9, 14 and 30 is bus number 1 and for the 118 bus bar system is bus number 69. When there is no variation in the three phases, it means that the generator is not close to the compensation point and does not require any action. Figure 7 shows the response of the generators to the reactive power needs of the EPS, for the 14, 30 and 118 bus-bar systems it can be seen that the slack generator has negative values

of reactive power; this is because the characteristics of the systems cause reagents to be delivered, which does not happen in the 9 bus bar system, due to its relative simplicity.

Table 2, as stated above, describes a summary of which bus compensation was located and its value in Mvar. These values were selected depending on the needs of the electrical system, since the greater the reactive power value in Mvar, the greater the variation in the results and, for safety reasons, standard reactive values for compensation were chosen for each IEEE electrical system, considering an independent control of the firing angle for each of the phases.

4.2. Real-Case Results of the 230 kV Ecuador Line

The methodology was tested on the 230 kV system in Ecuador, a system that is georeferenced unlike the IEEE test systems. In Figure 8, it can be seen where the model will locate reactive compensation; this is the "El Inga" substation, where the results meet expectations. In the same way, the latitude and longitude where desired changes must be taken into account work and obtain the data of the electrical system in order to carry out compensation planning in countries where it is desired to use a certain technology.
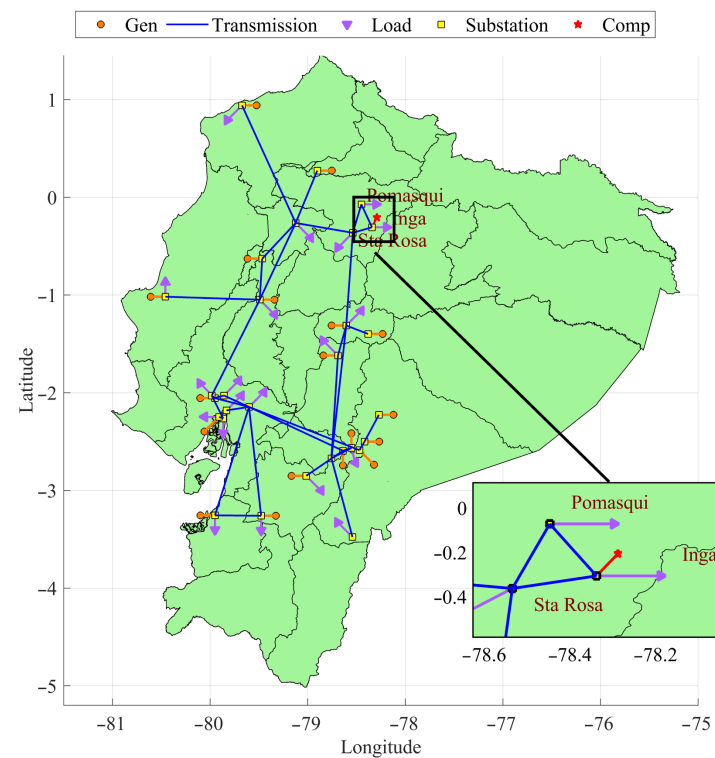

Figure 8. Location of compensation in the Ecuador case.

The voltage results can be seen in Figure 9; likewise, before the compensation, the unbalance is observed in the three phases of the "El Inga" substation since they have different magnitudes, However, after the compensation, the magnitude of the three phases are equalized, correcting the unbalance. The compensation value that was entered was 10 Mvar, obtaining a voltage increase from 0.94 to 0.95, entering the range of ±5% in the voltage level.

For the results of the flow of the transmission lines, a number had to be assigned to each substation as can be seen in the Table 1, where the name of the substation is detailed with its bus number. Figure 10 denotes the flow of reactive energy in the transmission lines of the 230 kV network in Ecuador when there is no compensation and when there is compensation, varying the magnitude in the lines near the place where it occurs. In lines 1–2, 1–5, 2–5 and 4–5, a change in magnitude is denoted; this is due to the proximity to the place of compensation.
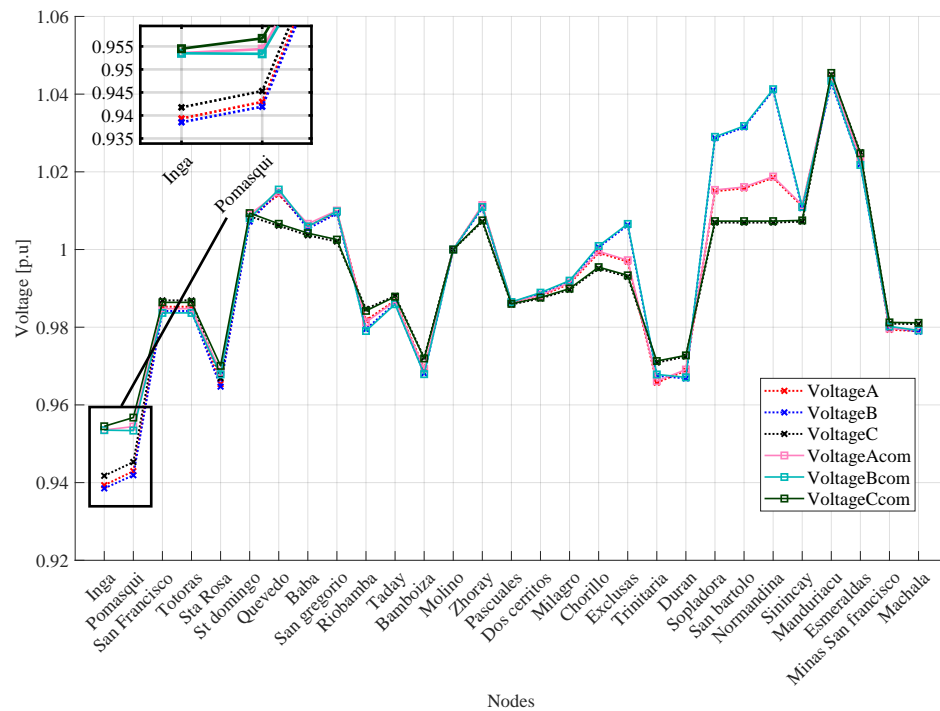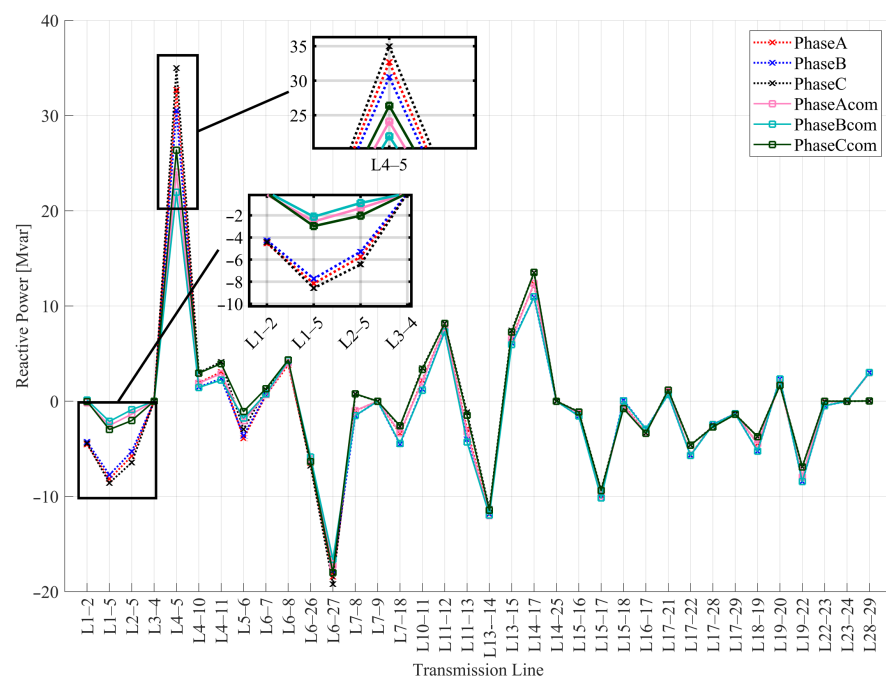
Figure 9. Voltage magnitude.

Figure 10. Reactive power of transmission lines.

By applying the model to the electrical system of Ecuador, solutions that go hand in hand with reality are obtained and, thus, guarantee the improvement in the same to obtain a more robust system.

The slack bus of the Ecuadorian system is number 13 which bears the name of "Molino" according to Table 1, which will be only for this case. In Figure 11, the dispatch of reactive power by the generators for their three phases when there is compensation and when there

is no compensation is shown, confirming that the results that vary with the action of the inclusion of compensation are the closest to said point.
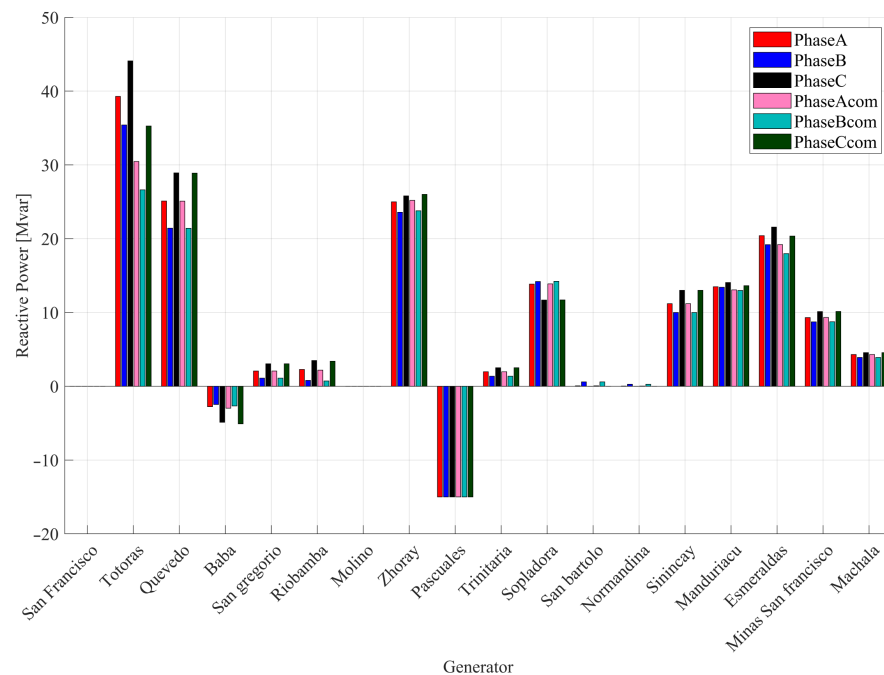

Figure 11. Dispatch of reactive power from generators.

5. Conclusions

Due to uncertainty in electrical demand, which often occurs in reality, there is an imbalance in the electrical network, which is why the model presented complies with the location of compensation in the electrical system, allowing the behaviour of the electrical variables to be observed, obtaining differences between when there is no compensation compared to when there is compensation, achieving favourable results and guaranteeing correct operation.

Optimal power-flow solutions are found when there is an imbalance in the network for any power system, so it follows that the model is flexible and then, through heuristics, correctly locates reactive compensation. This is the main contribution because the higher the value of compensation power, the greater the improvement in the electrical system. On the other hand, the heuristics allowed solution of the location of reactive compensation in all the cases presented, where it is shown that it would be scalable with measurable solutions.

The methodology complies with the operating ranges presented in the model restrictions allowing the results to comply with what is established, achieving a great impact as can be seen in the results of voltage profiles which were improved. In addition, the reduction in reactive power in the transmission lines makes the system stable, ensuring reliability in the SEP.

When verifying the behavior of the proposed methodology, it is observed that, in the nodes in which the parallel compensator is placed, the unbalance is reduced to 0%. A proposal for future research is the dynamic analysis of the EPS and, thereby, verification of the response of this methodology before changing demand scenarios.

Abbreviations

The abbreviations used in this article are as follows

Index

i, j, k	Índices de las barras
sh	Índice de compensación
t, h, d	Índice años, bloques y cargas eléctricas
ξ	Índice de escenarios
b	Índice de banco de capacitores estáticos

Parameters

P_{sh}, Q_{sh}	Potencia activa y reactiva del compensador
V_{sh}	Voltaje del compensador
θ_{sh}	Ángulo del compensador
G_{sh}	Conductancia del compensador
B_{sh}	Suceptancia del compensador
V_i	Voltaje de la barra
θ_i	Ángulo de la barra
PE	Intercambio de potencia activa
I_{sh}^{spec}	Corriente de control del compensador
S_{ij}	Flujo de potencia aparente
P_i^{cal}, Q_i^{cal}	Potencia activa y reactiva nodal calculada
CI, CO	Costo de inversión y costo de operación
C^{loss}	Voltage at bus bar j
ρ^{ξ}	Probabilidad del escenario
ΔD_t^{ξ}	Desconexión de carga total en el año t del escenario ξ
Ω_j	Conjunto de componentes conectados a la barra j
P_{ght}, Q_{ght}	Potencia de generación activa y reactiva de la unidad g en el bloque h del año t
P_{wht}	Despacho del generador w en el bloque h en el año t
P_{dht}, Q_{dht}	Carga activa y reactiva de la carga d en el bloque h en el año t
δ_{dht}^{ξ}	Desconexión de la carga activa en la carga d en el bloque h en el año t del escenario ξ
$P_{ij,ht}, Q_{ij,ht}$	Flujo de potencia activa y reactiva de la línea (i, j) del bloque h en el año t
Q_{bht}, Q_{shht}	Despacho de potencia reactiva del capacitor y compensador en el bloque h en el año t
y^b, z^b	Decisiones de despacho de acuerdo a información prevista
y^{ξ}, z^{ξ}	Decisiones de despacho en diferentes escenarios
C_e	Precio de electricidad
ζ	Horas de actividad de la carga máxima al año
$\Re_{SVC}$	Ubicaciones candidatas del SVC
C_{SVC}	Costo de inversión del SVC
Q_{SVC}	Capacidad de compensación
$Q_{i,t}^{SVC}$	Potencia del SVC en el tiempo t
E_i	Voltaje del generador i
$X'_{d,i}$	Reactancia transitoria eje directo
ω	Frecuencia angular
β	Ángulo de disparo SVC
a_g, b_g, c_g	coeficientes costo de la unidad de generación

References

1. Vitor, T.S.; Vieira, J.C.M. Operation planning and decision-making approaches for Volt/Var multi-objective optimization in power distribution systems. *Electr. Power Syst. Res.* **2021**, *191*, 106874. [CrossRef]
2. Fagundes, S.M.; Cardoso, F.L.; Stangler, E.V.; Neves, F.A.; Mezaroba, M. A detailed power flow analysis of the dual unified power quality conditioner (iUPQC) using power angle control (PAC). *Electr. Power Syst. Res.* **2021**, *192*, 106933. [CrossRef]
3. Karmakar, N.; Bhattacharyya, B. Optimal reactive power planning in power transmission network using sensitivity based bi-level strategy. *Sustain. Energy Grids Netw.* **2020**, *23*, 100383. [CrossRef]
4. Kraiczy, M.; Wang, H.; Schmidt, S.; Wirtz, F.; Braun, M. Reactive power management at the transmission-distribution interface with the support of distributed generators—A grid planning approach. *IET Gener. Transm. Distrib.* **2018**, *12*, 5949–5955. [CrossRef]
5. Liu, J.; Xu, Y.; Dong, Z.Y.; Wong, K.P. Retirement-Driven Dynamic VAR Planning for Voltage Stability Enhancement of Power Systems with High-Level Wind Power. *IEEE Trans. Power Syst.* **2018**, *33*, 2282–2291. [CrossRef]
6. Mi, Y.; Song, Y.; Fu, Y.; Wang, C. The Adaptive Sliding Mode Reactive Power Control Strategy for Wind-Diesel Power System Based on Sliding Mode Observer. *IEEE Trans. Sustain. Energy* **2020**, *11*, 2241–2251. [CrossRef]
7. Ding, T.; Yang, Q.; Yang, Y.; Li, C.; Bie, Z.; Blaabjerg, F. A data-driven stochastic reactive power optimization considering uncertainties in active distribution networks and decomposition method. *IEEE Trans. Smart Grid* **2018**, *9*, 4994–5004. [CrossRef]
8. Ettappan, M.; Vimala, V.; Ramesh, S.; Kesavan, V.T. Optimal reactive power dispatch for real power loss minimization and voltage stability enhancement using Artificial Bee Colony Algorithm. *Microprocess. Microsyst.* **2020**, *76*, 103085. [CrossRef]
9. Tahboub, A.M.; El Moursi, M.S.; Woon, W.L.; Kirtley, J.L. Multiobjective Dynamic VAR Planning Strategy with Different Shunt Compensation Technologies. *IEEE Trans. Power Syst.* **2018**, *33*, 2429–2439. [CrossRef]
10. Shojaei, A.H.; Ghadimi, A.A.; Miveh, M.R.; Gandoman, F.H.; Ahmadi, A. Multiobjective reactive power planning considering the uncertainties of wind farms and loads using Information Gap Decision Theory. *Renew. Energy* **2021**, *163*, 1427–1443. [CrossRef]
11. Dike, D.O.; Mahajan, S.M. Voltage stability index-based reactive power compensation scheme. *Int. J. Electr. Power Energy Syst.* **2015**, *73*, 734–742. [CrossRef]
12. Frolov, V.; Thakurta, P.G.; Backhaus, S.; Bialek, J.; Chertkov, M. Operations- and uncertainty-aware installation of FACTS devices in a large transmission system. *IEEE Trans. Control Netw. Syst.* **2019**, *6*, 961–970. [CrossRef]
13. Ranganathan, S.; Venugopal, E.; Kannan, C. *Multi-Objectives for TCSC Placement Using Self-Adaptive Firefly Algorithm*; Springer: Singapore, 2022; pp. 477–489. [CrossRef]
14. Khan, N.H.; Wang, Y.; Tian, D.; Jamal, R.; Iqbal, S.; Saif, M.A.A.; Ebeed, M. A Novel Modified Lightning Attachment Procedure Optimization Technique for Optimal Allocation of the FACTS Devices in Power Systems. *IEEE Access* **2021**, *9*, 47976–47997. [CrossRef]
15. Zhou, Z.; He, C.; Liu, T.; Dong, X.; Zhang, K.; Dang, D.; Chen, B. Reliability-Constrained AC Power Flow-Based Co-Optimization Planning of Generation and Transmission Systems With Uncertainties. *IEEE Access* **2020**, *8*, 194218–194227. [CrossRef]
16. Todescato, M.; Simpson-Porco, J.W.; Dorfler, F.; Carli, R.; Bullo, F. Online distributed voltage stress minimization by optimal feedback reactive power control. *IEEE Trans. Control Netw. Syst.* **2018**, *5*, 1467–1478. [CrossRef]
17. Pires, V.F.; Pombo, A.V.; Lourenço, J.M. Multi-objective optimization with post-pareto optimality analysis for the integration of storage systems with reactive-power compensation in distribution networks. *J. Energy Storage* **2019**, *24*, 100769. [CrossRef]
18. Liudvinavičius, L. Compensation of Reactive Power of AC Catenary System. *Procedia Eng.* **2017**, *187*, 185–197. [CrossRef]
19. Shefaei, A.; Vahid-Pakdel, M.J.; Mohammadi-ivatloo, B. Application of a hybrid evolutionary algorithm on reactive power compensation problem of distribution network. *Comput. Electr. Eng.* **2018**, *72*, 125–136. [CrossRef]
20. Yang, D.; Cheng, H.; Ma, Z.; Yao, L.; Zhu, Z. Dynamic VAR planning methodology to enhance transient voltage stability for failure recovery. *J. Mod. Power Syst. Clean Energy* **2018**, *6*, 712–721. [CrossRef]
21. Amrane, Y.; Boudour, M.; Belazzoug, M. A new Optimal reactive power planning based on Differential Search Algorithm. *Int. J. Electr. Power Energy Syst.* **2015**, *64*, 551–561. [CrossRef]
22. Carrión, D.; García, E.; Jaramillo, M.; González, J.W. A Novel Methodology for Optimal SVC Location Considering N-1 Contingencies and Reactive Power Flows Reconfiguration. *Energies* **2021**, *14*, 6652. [CrossRef]
23. Khan, N.H.; Wang, Y. Optimal Siting and Sizing of SSSC Using Modified Salp Swarm Algorithm Considering Optimal Reactive Power Dispatch Problem. *IEEE Access* **2021**, *9*, 49249–49266. [CrossRef]
24. Mahdad, B. Optimal reconfiguration and reactive power planning based fractal search algorithm: A case study of the Algerian distribution electrical system. *Eng. Sci. Technol. Int. J.* **2019**, *22*, 78–101. [CrossRef]
25. Korunovic, L.M.; Jovic, A.S.; Djokic, S.Z. Field-Based Evaluation of the Effects of Shunt Capacitors on the Operation of Distribution Transformers. *IEEE Trans. Power Deliv.* **2019**, *34*, 680–689. [CrossRef]
26. Ferreira, S.C.; Gonzatti, R.B.; Pereira, R.R.; Da Silva, C.H.; Da Silva, L.E.; Lambert-Torres, G. Finite control set model predictive control for dynamic reactive power compensation with hybrid active power filters. *IEEE Trans. Ind. Electron.* **2018**, *65*, 2608–2617. [CrossRef]
27. Arulraj, R.; Kumarappan, N. Optimal economic-driven planning of multiple DG and capacitor in distribution network considering different compensation coefficients in feeder's failure rate evaluation. *Eng. Sci. Technol. Int. J.* **2019**, *22*, 67–77. [CrossRef]
28. Wang, J.; Zhou, N.; Chung, C.Y.; Wang, Q. Coordinated Planning of Converter-Based DG Units and Soft Open Points Incorporating Active Management in Unbalanced Distribution Networks. *IEEE Trans. Sustain. Energy* **2020**, *11*, 2015–2027. [CrossRef]

29. El-Azab, M.; Omran, W.A.; Mekhamer, S.F.; Talaat, H.E.A. Allocation of FACTS Devices Using a Probabilistic Multi-Objective Approach Incorporating Various Sources of Uncertainty and Dynamic Line Rating. *IEEE Access* **2020**, *8*, 167647–167664. [CrossRef]

30. Zeinalzadeh, A.; Mohammadi, Y.; Moradi, M.H. Optimal multi objective placement and sizing of multiple DGs and shunt capacitor banks simultaneously considering load uncertainty via MOPSO approach. *Int. J. Electr. Power Energy Syst.* **2015**, *67*, 336–349. [CrossRef]

31. Garces, A. A Linear Three-Phase Load Flow for Power Distribution Systems. *IEEE Trans. Power Syst.* **2016**, *31*, 827–828. [CrossRef]

32. Wang, Y.; Zhang, N.; Li, H.; Yang, J.; Kang, C. Linear three-phase power flow for unbalanced active distribution networks with PV nodes. *CSEE J. Power Energy Syst.* **2017**, *3*, 321–324. [CrossRef]

33. Kim, Y.J. Development and Analysis of a Sensitivity Matrix of a Three-Phase Voltage Unbalance Factor. *IEEE Trans. Power Syst.* **2018**, *33*, 3192–3195. [CrossRef]

34. Liu, Z.; Milanović, J.V. Probabilistic Estimation of Voltage Unbalance in MV Distribution Networks With Unbalanced Load. *IEEE Trans. Power Deliv.* **2015**, *30*, 693–703. [CrossRef]

35. Cheung, V.S.P.; Chung, H.S.H.; Wang, K.W.; Lo, A.W.L. Paralleling multiple static synchronous series compensators using daisy-chained transformers. *IEEE Trans. Power Electron.* **2014**, *29*, 2764–2773. [CrossRef]

36. Monemi Bidgoli, M.; Karimi, H.; Jadid, S.; Anvari-Moghaddam, A. Stochastic electrical and thermal energy management of energy hubs integrated with demand response programs and renewable energy: A prioritized multi-objective framework. *Electr. Power Syst. Res.* **2021**, *196*, 107183. [CrossRef]

37. Mao, X.; Zhu, W.; Wu, L.; Zhou, B. Optimal allocation of dynamic VAR sources using zoning-based distributed optimization algorithm. *Int. J. Electr. Power Energy Syst.* **2019**, *113*, 952–962. [CrossRef]

38. Masache, P.; Carrión, D.; Cárdenas, J. Optimal transmission line switching to improve the reliability of the power system considering ac power flows. *Energies* **2021**, *14*, 3281. [CrossRef]